

ANTIOXIDANT PROPERTIES AND BINDING INTERACTIONS
OF 1-MORPHOLIN-4-YL-3-{[2-(3-NITROPHENYL)-2-OXOETHYL]THIO}-
5,6,7,8-TETRAHYDROISOQUINOLINE-4-CARBONITRILE
WITH BOVINE SERUM ALBUMIN

K. R. GRIGORYAN ^{1*}, A. V. IGITYAN ^{1**}, H. H. VARDANYAN ^{2***},
Zh. G. KHACHATRYAN ^{3****}, A. S. HARUTYUNYAN ^{2*****}, A. L. ZATIKYAN ^{1*****},
H. A. SHILAJYAN ^{1*****}

¹ Laboratory of Physical Chemistry, Chemistry Research Center, YSU, Armenia

² Scientific Technological Center of Organic and Pharmaceutical Chemistry of
NAS of the RA, Institute of Fine Organic Chemistry of A.L. Mnjoyan, Armenia

³ A. B. Nalbandyan Institute of Chemical Physics, NAS of the RA, Armenia

The binding interactions of newly designed/synthesized 1-morpholin-4-yl-3-
{[2-(3-nitrophenyl)-2-oxoethyl]thio}-5,6,7,8-tetrahydroisoquinoline-4-carbonitrile
(C1) with transporting protein bovine serum albumin (BSA) were studied using
UV/Vis and FTIR spectroscopy methods. The antioxidant properties of C1 were
evaluated using DPPH[·] assay. FTIR spectra deconvolution of BSA amide I band
(1600–1700 cm^{-1}) was used to analyze changes in the secondary structure of BSA
upon binding with C1. It was shown that C1 binds to BSA reversibly with
 $K_B = (3.52 \pm 0.01) \cdot 10^5 M^{-1}$ and the binding induces pronounced changes in the
secondary structure of BSA. The obtained results demonstrate that C1 can be
characterized as a compound with high radical (DPPH[·]) scavenging capacity.

<https://doi.org/10.46991/PYSUB.2025.59.3.057>

Keywords: tetrahydroisoquinoline-4-carbonitrile, antioxidant, DPPH radical,
bovine serum albumin, UV/Vis, FTIR.

Introduction. Aging, rheumatoid arthritis, neurodegenerative, cardiovascular,
cancer, and many other diseases are caused by the action of free radicals damaging
cells. That is why nowadays great attention is paid to antioxidants (natural and
synthetic) that can scavenge and neutralize free radicals [1–5]. Isoquinoline-4-
carbonitriles are not only accessible intermediates for organic synthesis, but also
represent privileged scaffolds in medicinal chemistry. These synthetic compounds
have been employed in a wide range of research areas, notably as intermediates in
the synthesis of pharmaceuticals and agrochemicals. Their structural features make
them valuable in drug discovery, particularly for targeting neurological disorders.

* E-mail: kara@ysu.am

**** E-mail: harutyunyan_arp@mai.ru

** E-mail: ani_igityan@ysu.am

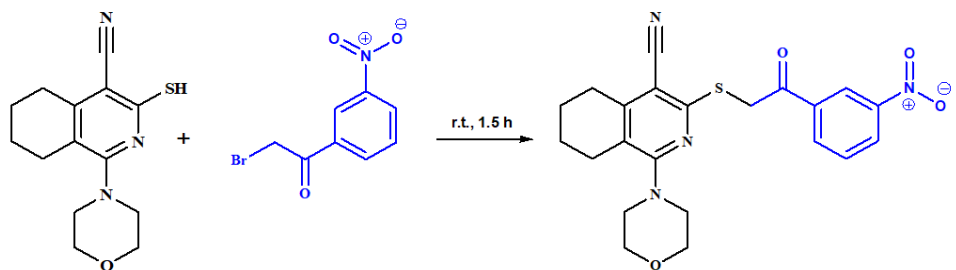
***** E-mail: ashkhen@ysu.am

*** E-mail: vardanyanhexine63@gmail.com

***** E-mail: hshilajyan@ysu.am

**** E-mail: janya.khachatryan@ichph.sci.am

Applications extend further into material science, biochemistry, and analytical chemistry [6]. The tetrahydroisoquinoline ring system is a core structure found in many naturally occurring alkaloids, second in abundance only to indole alkaloids [7, 8]. Compounds containing this moiety serve as precursors in the synthesis of alkaloids, enzyme inhibitors, fungicides, potassium channel blockers, and drugs intended for the treatment of cardiovascular diseases, bronchial asthma, cancer, and viral infections. Additionally, derivatives of tetrahydroisoquinoline have demonstrated anticonvulsant, antibacterial, neurotropic, and antimicrobial activities [9–11]. On the other hand, many nitro-substituted compounds are another important class of bioactive molecules, known for their versatile biochemical and pharmacological (anticancer and antioxidant) applications [12, 13]. Antiradicals are defined as substances that at relatively low concentrations can significantly inhibit the oxidation processes of the targets. Transport of these compounds in living cells could be performed by binding with carrier proteins. Human serum albumin (HSA) and bovine serum albumin (BSA) are commonly used as model proteins in biopharmaceutical studies. These proteins are responsible for transporting and distributing many endogenous and exogenous substances. HSA and BSA display approximately similar structures and functional properties [14]. BSA possesses spectral (UV/Vis, fluorescence, IR) properties due to the presence of aromatic amino acids phenylalanine (Phe), tyrosine (Tyr), tryptophan (Trp) residues, and amide groups. By monitoring the absorption of BSA, binding affinities (binding mechanism, binding mode, binding constants, binding sites, etc.) and structural changes in the BSA secondary structure could be determined [15–19]. Taking into account these facts, we synthesized new derivatives incorporating two pharmacophore moieties, nitrophenyl and pyridine, as a hybrid molecule. This work presents studies on the antioxidant properties, binding interactions of 1-morpholin-4-yl-3-{[2-(3-nitrophenyl)-2-oxoethyl]thio}-5,6,7,8-tetrahydroisoquinoline-4-carbonitrile (C1) (see Scheme) with carrier protein BSA and FTIR analysis of conformational changes in the secondary structure of protein caused by the binding with C1. These results may contribute to the development of improved bioactive molecules based on the nitrophenyl-containing tetrahydroisoquinoline scaffold.



Scheme. Synthesis of 1-morpholin-4-yl-3-{[2-(3-nitrophenyl)-2-oxoethyl]thio}-5,6,7,8-tetrahydroisoquinoline-4-carbonitrile (C1).

Materials and Methods.

Materials. BSA (lyophilized powder) and DPPH⁺ were purchased from “Sigma-Aldrich” (USA) and used without further purification. All other chemicals were of analytic grade. The structure of C1 ($C_{22}H_{22}N_4O_4S$) was confirmed by IR and

NMR spectroscopy, HRMS, and elemental analysis. ^1H - and ^{13}C -NMR spectra were recorded in $\text{DMSO}-d_6/\text{CCl}_4$, v/v solution (300 MHz for ^1H and 75.462 MHz for ^{13}C) on a Varian mercury spectrometer (Varian Inc., Palo Alto, CA, USA). The coupling constants (J) are given in Hertz. Chemical shifts are reported as δ (parts per million) relative to TMS (tetramethylsilane) as an internal standard. IR spectra were recorded on a Nicolet Avatar 330-FTIR spectrophotometer (“Thermo Nicolet”, Foster, CA, USA) and the reported wave numbers are given in cm^{-1} . Elemental analysis was performed on a Euro EA 3000 Elemental Analyzer (“EuroVector”, Pavia, Italy). ESI-MS spectra were measured with a MicroTof instrument (“Bruker Daltonics”, Billerica, MA, USA). TLC analysis was performed on Xtra SIL G/UV254 plates (“Macherey-Nagel”, Düren, German). Melting points were determined on an MP420 melting point apparatus. They are expressed in degrees centigrade ($^{\circ}\text{C}$).

Methods.

Synthesis of 1-Morpholin-4-yl-3-{{[2-(3-nitrophenyl)-2-oxoethyl]thio}-5,6,7,8-tetrahydroisoquinoline-4-carbonitrile (C1). To a solution of 1-morpholin-4-yl-3-thioxodehydroisoquinoline-4-carbonitrile [19] (2.75 g, 0.01 mol) in 20 mL of aqueous sodium carbonate (Na_2CO_3 , 1.06 g, 0.01 mol), 2-bromo-1-(4-nitrophenyl)ethan-1-one (2.44 g, 0.01 mol) was added. The reaction mixture was stirred at room temperature for 1.5 h. The resulting precipitate was filtered, washed with water, dried, and recrystallized from ethanol. NMR and LC-MS spectra of C1 are presented below. C1 is a yellow solid; yield 74.1%; m.p. 127.6–128.0 $^{\circ}\text{C}$; R_f =0.58 (chloroform:ethanol = 3:2); IR, ν/cm^{-1} : 2223 (C≡N), 1640 (C=O), 1580 (C=Car), 1537 (N-Oasym), 1358 (N-Osym).

^1H NMR (δ , ppm, Hz) (DMSO- d_6): 1.69 m (2H, 7- CH_2); 1.83 m (2H, 6- CH_2); 2.68 m (2H, 5- CH_2); 2.84 m (2H, 8- CH_2); 3.09 m (4H, N(CH_2)₂); 3.56 m (4H, O(CH_2)₂); 4.82 s (2H, SCH₂); 7.82 t (1H, J = 7.1, α -Ph CH); 8.44 dd (2H, J_1 = 9.6, J_2 = 1.8, α' , γ -Ph CH); 8.77 t (1H, J = 2.0, β' -Ph CH).

^{13}C NMR (75 MHz , DMSO- d_6 , 1/3): δ 18.12, 26.10, 28.06, 28.56, 48.35, 50.73, 52.77, 53.78, 61.75, 75.38, 75.41, 82.81, 110.25, 114.58, 126.58, 127.68, 128.20, 137.42, 150.27, 158.16, and 159.31.

Anal. calc. for $\text{C}_{22}\text{H}_{22}\text{N}_4\text{O}_4\text{S}$: C 60.26; H 5.06; N 12.78 and S 7.31%. Found: C 60.18; H 5.17; N 12.97 and S 7.49%. HRMS (ESI) of $\text{C}_{22}\text{H}_{22}\text{N}_4\text{O}_4\text{S}$, m/z : calculated for 439.14 [M + H]⁺, found: 439.1443.

UV/Vis Spectroscopy Studies.

DPPH Radical-Scavenging Assay. DPPH radical scavenging by C1 was studied using DPPH radical-scavenging assay. The DPPH[·], with an odd electron delocalized over the molecule, shows a strong absorption band at 516 nm in ethanol. The scavenging of DPPH[·] by antioxidants is achieved by donating H-atom to form the stable DPPH-H molecule, causing decrease in absorbance due to solution color changing from purple to yellow. The stock solution of DPPH[·] was prepared in ethanol, and the initial concentration was determined using UV/Vis spectra absorption at 516 nm with the molar absorption coefficient ε =12509 $M^{-1}\cdot\text{cm}^{-1}$ [20]. The stock solution of C1 was prepared in ethanol with an initial concentration of $1.0\cdot 10^{-2} \text{ mL}^{-1}$ (weight method). C1 was added to the DPPH[·] solution, kept in the dark place for 30 min and after the absorption was measured in the 200–600 nm wavelength range. Electronic absorption spectra of solutions were registered on a

spectrophotometer Specord 50PC (Germany). The radical scavenging capacity (R_S) of C1 was calculated using (Eq. 1):

$$R_S = \frac{A_0 - A_S}{A_0} \cdot 100\%, \quad (1)$$

where A_0 is the absorbance of the sample in the absence and A_S in the presence of C1, respectively.

Binding of C1 to BSA. The stock solution of BSA was prepared in double distilled water and stored at 4°C. The concentration of BSA (0.4 mg/mL) was determined using UV/Vis spectra absorption at 278 nm with the molar absorption coefficient $\varepsilon=43.820 M^{-1} \cdot cm^{-1}$ [21]. With gentle stirring, aliquots (10 μ L) of C1 solution ($1.6 \cdot 10^{-4} M$) were added to BSA solution and the spectra were registered on a spectrophotometer Specord 50PC (Germany) in the range of 200–400 nm.

FTIR Spectra. FTIR spectra of BSA solutions were recorded on a Nicolet iS50 FT-IR spectrometer using ATR attachment with a diamond crystal, in the range of 4000–400 cm^{-1} , with a resolution of 4 cm^{-1} and a number of scans 32. Gauss-Lorentz mixed function of the LinkFit program was used for the identification of the secondary structure elements and conformational changes of the protein. The different types of conformational and transformational species were confirmed by the analysis of observed peak frequencies. The peak frequency set was preliminarily deduced by the second derivative method [22, 23]. The percentage of secondary structure elements was calculated from the integrated areas of the deconvoluted spectra. The absolute error of the analysis is 1%.

Data Analysis. All experiments and measurements were carried out in triplicate. Data analysis and graphing were performed by OriginPro 8.5 and Excel 2010 software.

Results and Discussion.

UV/Vis Spectroscopy Studies.

Binding Interactions of C1 to BSA. UV/Vis spectroscopy was used to determine binding interaction of C1 to BSA. UV/Vis spectra of BSA in the presence of C1 are presented in Fig. 1.

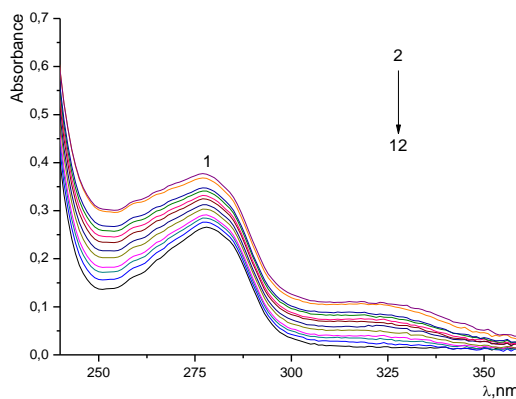


Fig. 1. UV/Vis spectra of BSA in the presence of C1: 1 – BSA; 2–12 – BSA–C1.
[C1] = $0.53\text{--}6.93 \cdot 10^{-6} M$. [BSA] = 0.4 mg/mL.

Binding of C1 to BSA resulted in absorbance decrease due to higher molar absorption coefficient of formed BSA–C1 complex. The apparent dissociation constant (K_D) of the complex was determined using the equation presented below:

$$\frac{1}{\Delta A} = \frac{K_D}{\Delta A_\infty} \cdot \frac{1}{[S]} + \frac{1}{\Delta A_\infty}, \quad (2)$$

where ΔA presents the difference of BSA absorption in the presence and absence of C1, $[S]$ is the concentration of free C1, which is assumed to be equal to its initial concentration, and ΔA_∞ is the absorbance of the completely formed adduct. Using these values, the binding constant (K_B) was calculated from the equation $K_B = \frac{1}{K_D}$.

Fig. 2 presents the dependence of $\frac{1}{\Delta A}$ on $\frac{1}{[S]}$.

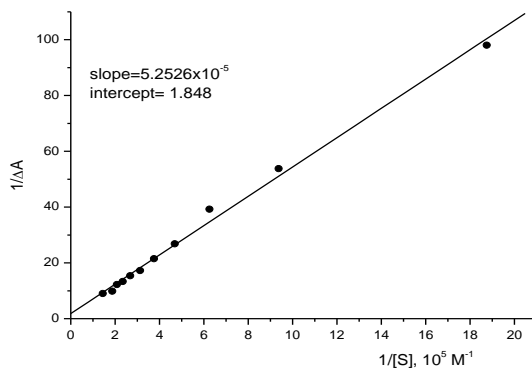


Fig. 2. The dependence of $1/\Delta A$ on $1/[S]$.

Hill coefficient (h), which shows the binding mode between C1 and the protein, was determined from the logarithmic form of the Hill equation presented below:

$$\log \frac{\Delta A}{\Delta A_\infty - \Delta A} = h \log[S] + \log K_D, \quad (3)$$

where ΔA_∞ and K_D were calculated from the dependence of $\frac{1}{\Delta A}$ on $\frac{1}{[S]}$ [24, 25].

Table 1

Dissociation constant (K_D), binding constant (K_B), Hill coefficient (h) for the BSA–C1 complex

Parameter	K_D, M	K_B, M^{-1}	h
	$(2.84 \pm 0.01) \cdot 10^{-4}$	$(3.52 \pm 0.01) \cdot 10^5$	$0.99 (\pm 0.01)$

Table 2

Radical scavenging capacity (Rs) data at different concentrations of C1

$Rs, \%$	2.9	6.8	8.9	14.5	18.5	22.8	28.8
$[C1] \cdot 10^6, M$	1.07	2.13	3.20	4.27	5.33	5.97	6.93

Note: EC₁₀₀ was not determined due to C1 limited solubility in aqueous media.

Obtained results show that C1 binds to BSA with a typical for transporting proteins association constant in the range of 10^4 – 10^6 M^{-1} with a single mode of association. Usually, drugs bind to one or very few high-affinity sites of albumins with above-mentioned typical association constants [26]. From the results presented in Tab. 2, it can be concluded that C1 is endowed with high radical (DPPH[·]) scavenging capacity.

FTIR Spectra Analysis. Vibrational spectroscopy methods, such as FTIR, Raman and CD, are important and commonly used techniques for protein structure and dynamics studies. FTIR spectroscopy application to protein secondary structure analysis, conformational changes, structural dynamics and stability are discussed in [27]. Nine FTIR absorption bands characterizing protein structure (amide A, B, and amide I–VII) were described in detail by Bunker et al. [28]. Of these, the amide I and II bands are the most prominent vibrational bands of the protein backbone. For the qualitative and quantitative analysis of the secondary structure components of the protein amide I band (1600 – 1700 cm^{-1}) corresponding mainly to C=O stretching vibrations of the peptide linkages is used. Amide II band (1500 – 1600 cm^{-1}) derives mainly from the N–H bending (40–60% of the potential energy) and C–N stretching vibration (18–40%), which shows much less protein conformational sensitivity than its amide I band [28, 29]. The FTIR spectra of BSA amide I band in 1600 – 1700 cm^{-1} region are presented in Fig. 3.

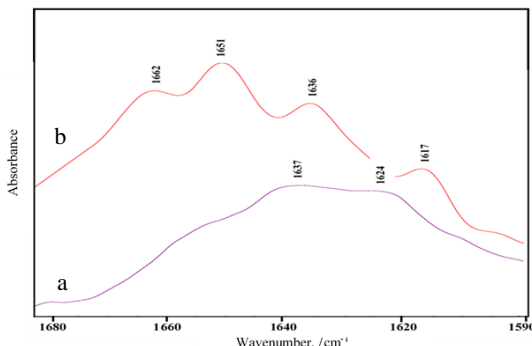


Fig. 3. FTIR spectra of the amide I band of BSA (a) and BSA–C1 (b).
 $[\text{BSA}] = 0.4\text{ mg/mL}$, $[\text{C1}] = 6.0 \cdot 10^{-5}\text{ M}$.

Two well expressed peaks characterize the amide I band of BSA in bidistilled water: at 1637 and 1624 cm^{-1} . Upon addition of C1 to BSA solution, four peaks shifted to higher vibrational region (at 1662 , 1651 , 1636 and 1617 cm^{-1}) are observed in FTIR spectra of the amide I band. The qualitative and quantitative analysis of the secondary structure components of BSA as a result of complex formation with C1, is carried out by the deconvolution of amide I band (1700 – 1600 cm^{-1}) into separate components (Fig. 4, Tab. 3).

The curve fitting of amide I stretching region for BSA results in six components, which describe BSA secondary structure components: α -helices, β -structures (free, parallel, antiparallel, oligomer, β -sheets, β -turn) random coil and aromatic ring. Binding interactions of C1 to BSA results in changes in frequencies and band areas. A new component is observed at 1656 cm^{-1} which could be attributed to a part

of α -helices with weakened (may be unfolded) structure, caused by the rearrangement of the polypeptide carbonyl hydrogen-bonded species and finally leaded to the reduction of the protein helical structure. The percentage of β -sheet parallel structure increases, other forms of β -sheet structures decrease, random coil structures increase, and β -turn forms remain unchanged. So, the secondary structure of BSA is changed partially.

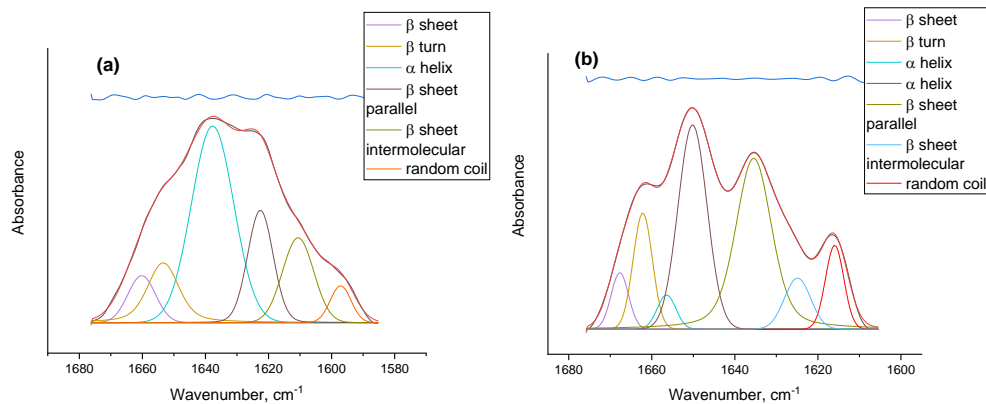


Fig. 4. Deconvoluted FTIR spectra of the amide I band of free- (a) and C1-bound BSA (b).
[BSA] = 0.4 mg/mL, [C1] = $6.0 \cdot 10^{-5}$ M.

Table 3

FTIR analysis of the amide I band of free and C1-bound BSA in bidistilled water. BSA – 0.4 mg/mL, C1 – $6.0 \cdot 10^{-5}$ M

Secondary structure component	Free BSA		C1-bound BSA	
	ν/cm^{-1}	% ($\pm 1\%$)	ν/cm^{-1}	% ($\pm 1\%$)
β-Sheet	1660	7.7	1668	5.2
β-Turn	1653	11.4	1662	11.7
α-Helix	–	–	1656	3.4
α-Helix	1638	42.8	1650	31.2
β-Sheet parallel	1622	21.7	1635	33.3
β-Sheet intermolecular	1609	11.7	1625	7.1
Random coil	1597	4.7	1616	8.1

Conclusion. UV/Vis and FTIR studies on binding interactions of C1 to BSA showed a reversible and single mode association mechanism of C1 to BSA with pronounced changes in secondary structure. The antioxidant properties of newly designed C1 can be characterized as a compound with high radical (DPPH[·]) scavenging capacity.

This work was supported by the Higher Education and Science Committee of the MESCS RA, in the frames of the research project YSU-CHEM.

Received 17.05.2025
Reviewed 25.06.2025
Accepted 07.07.2025

REFERENCES

1. Losada-Barreiro S., Bravo-Díaz C. Free Radicals and Polyphenols: The Redox Chemistry of Neurodegenerative Diseases. *Eur. J. Med. Chem.* **133** (2017), 379–402.
<https://doi.org/10.1016/j.ejmech.2017.03.061>
2. Butterfield A.D. Oxidative Stress in Neurodegenerative Disorders. *Antiox. Redox Sign.* **8** (2006), 1971–1973.
<https://doi.org/10.1089/ars.2006.8.1971>
3. Niedzielska E., Smaga I., et al. Oxidative Stress in Neurodegenerative Diseases. *Mol. Neurobiol.* **53** (2016), 4094–4125.
<https://doi.org/10.1007/s12035-015-9337-5>
4. Barnett J.B., Wang G.C., et al. Effect of the Radical Remission Multimodal Intervention on Quality of Life of People with Cancer Integrative Cancer Therapies. *Integr. Cancer Therap.* **23** (2024), 4–18.
<https://doi.org/10.1177/15347354241293197>
5. Fearon I.M., Faux S.P. Oxidative Stress and Cardiovascular Disease: Novel Tools Give (free) Radical Insight. *J. Molec. Cell. Cardiol.* **47** (2009), 372–381.
<https://doi.org/10.1016/j.yjmcc.2009.05.013>
6. Rode H.B., Sos M.L., et al. Synthesis and Biological Evaluation of 7-Substituted-1-(3-bromophenylamino)isoquinoline-4-carbonitriles as Inhibitors of Myosin Light Chain Kinase and Epidermal Growth Factor Receptor. *Bioorg. & Med. Chem.* **19** (2010), 429–439.
<https://doi.org/10.1016/j.bmc.2010.11.007>
7. Yang X., Miao X., et al. Isolation, Biological Activity, and Synthesis of Isoquinoline Alkaloids. *Natur. Prod. Rep.* **41** (2024), 1652–1722.
<https://doi.org/10.1039/d4np00023d>
8. Diaz G., Miranda I.L., Diaz M.A.N. *Quinolines, Isoquinolines, Angustureine, and Congeneric Alkaloids – Occurrence, Chemistry, and Biological Activity, Phytochemicals – Isolation, Characterisation and Role in Human Health* (2015).
<https://doi.org/10.5772/59819>
9. Tanwar A.K., Sengar N., Tetrahydroisoquinolines – an Updated Patent Review for Cancer Treatment (2016 – present). *Expert Opinion on Therapeutic Patents* **34** (2024), 873–906.
<https://doi.org/10.1080/13543776.2024.2391288>
10. Rasool F., Kumar B.K., et al. Medicinal Chemistry Perspectives of 1,2,3,4-Tetrahydroisoquinoline Analogs – Biological Activities and SAR Studies. *RSC Advances* **11** (2021), 12254–12287.
<https://doi.org/10.1039/d1ra01480c>
11. Sayed E.M., Bakhite E.A., et al. Novel Tetrahydroisoquinolines as DHFR and CDK2 Inhibitors: Synthesis, Characterization, Anticancer Activity and Antioxidant Properties. *BMC Chemistry* **18** (2024).
<https://doi.org/10.1186/s13065-024-01139-w>
12. Sayed E.M., Hassanien R., et al. Nitrophenyl-Group-Containing Heterocycles. I. Synthesis, Characterization, Crystal Structure, Anticancer Activity, and Antioxidant Properties of Some New 5,6,7,8-Tetrahydroisoquinolines Bearing 3(4)-Nitrophenyl Group. *ACS Omega* **7** (2022), 8767–8776.
<https://doi.org/10.1021/acsomega.1c06994>
13. Nandikolla A., Khetmalis Y.M., et al. Tetrahydroisoquinoline Based 5-Nitro-2-furoic Acid Derivatives: A Promising New Approach for Anti-Tubercular Agents. *New Journal of Chemistry* **47** (2023), 15378–15389.
<https://doi.org/10.1039/d3nj01907a>
14. Peters T. *All about Albumin Biochemistry. Genetics and Medical Applications*. CA, San Diego, Academic Press (1996), 432.
15. Kong J., Yu S. Fourier Transform Infrared Spectroscopic Analysis of Protein Secondary Structures. *Acta Biochim. Biophys. Sinica* **39** (2007), 549–559.
<https://doi.org/10.1111/j.1745-7270.2007.00320.x>
16. Grigoryan K., Shilajyan H., et al. Effect of Bovine Serum Albumin on Gallic Acid and Tannic Acid Radical Scavenging Properties and Binding Kinetics with 2,2-Diphenyl-1-picrylhydrazyl. *Proc. Biochem.* **141** (2024), 30–38.
<https://doi.org/10.1016/j.procbio.2024.02.009>

17. Pelton J.T., McLean L.R. Spectroscopic Methods for Analysis of Protein Secondary Structure. *Anal. Biochem.* **277** (2000), 167–176.
<https://doi.org/10.1006/abio.1999.4320>
18. Grigoryan K., Zatikyan A., Shilajyan H. Effect of Monovalent Ions on the Thermal Stability of Bovine Serum Albumin in Dimethylsulfoxide Aqueous Solutions. Spectroscopic Approach. *J. Biomol. Struct. Dynamics* **39** (2021), 2284–2288.
<https://doi.org/10.1080/07391102.2020.1743759>
19. Paronikyan E.G., Mirzoyan G.V., et al. Synthesis and Antibacterial Activity of Pyrano-(thiopyrano)[3,4-c]pyridine-, 2,7-naphthyridine-, and 5,6,7,8-tetrahydro-isoquinoline-3(2h)-thione Derivatives. *Pharm. Chem. J.* **27** (1993), 759–762.
<https://doi.org/10.1007/BF00780403>
20. Brand-Williams W., Cuvelier M.E., Berset C. Use of a Free Radical Method to Evaluate Antioxidant Activity Lebensm. Wiss. u.-Technol. **28** (1995), 25–30.
<https://doi.org/0023-6438/95/010025>
21. Pace C.N., Vajdos F., et al. How to Measure and Predict the Molar Absorption Coefficient of a Protein. *Protein Sci.* **4** (1995), 2411–2423.
<https://doi.org/10.1002/pro.5560041120>
22. Murayama K., Tomida M. Heat-Induced Secondary Structure and Conformation Change of Bovine Serum Albumin Investigated by Fourier Transform Infrared Spectroscopy. *Biochem.* **43** (2004), 11526–11532.
<https://doi:10.1021/bi0489154>
23. Lorenz-Fonfria V.A. Infrared Difference Spectroscopy of Proteins: From Bands to Bonds. *Chem. Rev.* **120** (2020), 3466–3576.
<https://dx.doi.org/10.1021/acs.chemrev.9b00449>
24. Grigoryan K.R., Kazaryan A.G. Interaction of Dimethylsulfoxide and Diethylsulfoxide Complexes of Platinum (II) with Bovine Serum Albumin. *J. Appl. Spect.* **76** (2009), 637–640.
<https://doi.org/10.1007/s10812-009-9241-8>
25. Shiraz Z.A., Sohrabi N., et al. Spectroscopic Study and Molecular Simulation: Bovine Serum Albumin Binding with Anticancer Pt Complex of Amyldithiocarbamate Ligand. *Heliyon* **9** (2023), e20090.
<http://creativecommons.org/licenses/by/4.0/>
26. Kragh-Hansen U., Chuang V.T.G., Otagiri M. Practical Aspects of the Ligand-Binding and Enzymatic Properties of Human Serum Albumin. *Biol. Pharm. Bull.* **25** (2002), 695–704.
<https://doi.org/10.1248/bpb.25.695>
27. Kong J., Yu S. Fourier Transform Infrared Spectroscopic Analysis of Protein Secondary Structures. *Acta Biochim. Biophys. Sinica* **39** (2007), 549–559.
<https://doi.org/10.1111/j.1745-7270.2007.00320.x>
28. Banker J. Amide Modes and Protein Conformation. *Biochem. Biophys. Acta* **1120** (1992), 123–143.
[https://doi.org/10.1016/0167-4838\(92\)90261-b](https://doi.org/10.1016/0167-4838(92)90261-b)
29. Yang S., Zhang Q., et al. Progress in Infrared Spectroscopy as an Efficient Tool for Predicting Protein Secondary Structure. *Int. J. Biol. Macromol.* **206** (2022), 175–187.
<https://doi.org/10.1016/j.ijbiomac.2022.02.104>

Կ. Ռ. ԳՐԻԳՈՐՅԱՆ, Ա. Վ. ԻԳԻՏՅԱՆ, Հ. Հ. ՎԱՐԴԱՆՅԱՆ, Ժ. Գ. ԽԱՉԱՏՐՅԱՆ,
 Ա. Ս. ՀԱՐՈՒԹՅՈՒՆՅԱՆ, Ա. Լ. ԶԱՏԻԿՅԱՆ, Հ. Ա. ՇԻԼԱՅՅԱՆ

1-ՄՈՐՖՈԼԻՆ-4-ԻԼ-3-{{2-(3-ՆԻՏՐՈՓԵՆԻԼ)-2-ՕՔՍՈՒՔԻԼ]ՓԻՈ}-5,6,7,8-
 ՏԵՏՐՎԿԻԴՐՈՒԶՈՔԻՆՈԼԻՆ-4-ԿԱՐԲՈՆԻՏՐԻԼԻ ՀԱԿԱԾՈՔՍԻ-
 ԴԱՆՏԱՅԻՆ ՀԱՏԿՈՒԹՅՈՒՆՆԵՐԸ ԵՎ ՓՈԽԱՉԴԵՑՈՒԹՅՈՒՆՆԵՐԸ
 ՑՈՒԼԻ ՇԻՃՈՒԿԱՅԻՆ ԱԼԲՈՒՄԻՆԻ ՀԵՏ

Նոր մշակված/սինթեզված 1-մորֆոլին-4-իլ-3-{{2-(3-նիտրոֆենիլ)-2-
 օքսուքիլ]թիո}-5,6,7,8-տետրահիդրոնիզոքինուլին-4-կարբոնիտրիլի (C1) փոխ-

ազդեցությունները ցույի շիճուկային ալբումինի (ՑԾԱ) հետ ուսումնասիրվել է էլեկտրոնային կանման և ֆուլյե ձևափոխմամբ ինֆրակարմիր սպեկտրոսկոպիայի (FTIR) մեթոդներով: C1-ի հակաօրսիդանտային հատկությունները գնահատվել են DPPH[·] անալիզի միջոցով: ՑԾԱ-ի ամիդ I կանման (1600–1700 cm^{-1}) FTIR սպեկտրների տարրապուծելիությունն օգտագործվել է C1-ի հետ կապվելիս ՑԾԱ-ի երկրորդային կառուցվածքի փոփոխությունները գնահատելու համար: Ցույց է տրվել, որ C1-ը դարձելիորեն կապվում է ՑԾԱ-ի հետ ($K_B = (3.52 \pm 0.01) \cdot 10^5 \text{ M}^{-1}$), ինչի հետևանքով տեղի է ունենում ՑԾԱ-ի երկրորդային կառուցվածքի արտահայտված փոփոխություններ: Ստացված արդյունքները ցույց են տալիս, որ C1-ը կարող է բնութագրվել որպես ռադիկալականներ (DPPH[·]) որակություն ունեցող միացություն:

К. Р. ГРИГОРЯН, А. В. ИГИТЯН, Г. Г. ВАРДАНЯН, Ж. Г. ХАЧАТРЯН,
А. С. АРУТИОНЯН, А. Л. ЗАТИКЯН, А. А. ШИЛАДЖЯН

АНТИОКСИДАНТНЫЕ СВОЙСТВА И ВЗАИМОДЕЙСТВИЯ
1-МОРФОЛИН-4-ИЛ-3-{{2-(3-НИТРОФЕНИЛ)-2-ОКСОЭТИЛ]ТИО}-5,6,7,8-
-ТЕТРАГИДРОИЗОХИНОЛИН-4-КАРБОНИТРИЛА С БЫЧЬИМ
СЫВОРОТОЧНЫМ АЛЬБУМИНОМ

Взаимодействие недавно разработанного/синтезированного 1-морфолин-4-ил-3-{{2-(3-нитрофенил)-2-оксоЭтил]тио}-5,6,7,8-тетрагидроизохинолин-4-карбонитрила (C1) с бычьим сывороточным альбумином (БСА) изучено с помощью электронной абсорбционной и инфракрасной спектроскопии с преобразованием Фурье (FTIR). Антиоксидантные свойства C1 оценивали с помощью DPPH[·]-анализа. Разложение FTIR спектров БСА полосы амида I (1600–1700 cm^{-1}) было использовано для оценки изменений вторичной структуры белка при связывании с C1. Было показано, что C1 обратимо связывается с БСА ($K_B = (3.52 \pm 0.01) \cdot 10^5 \text{ M}^{-1}$), что приводит к выраженным изменениям вторичной структуры белка. Полученные результаты показывают, что C1 можно охарактеризовать как соединение с высокой способностью поглощать радикалы (DPPH[·]).